scientific reports

Check for updates

OPEN

Synthesis and effect of 4-acetylphenylamine-based imidazole derivatives on migration and growth of 3D cultures of breast, prostate and brain cancer cells

Božena Golcienė[1], Rita Vaickelionienė[1], Ugnė Endriulaitytė[2], Vytautas Mickevičius[1]✉ & Vilma Petrikaitė[2,3]✉

In this study, we have synthesized novel 4-acetophenone moiety-bearing functionalized imidazole derivatives containing S-, and N-ethyl substituents and evaluated their anticancer activity. Their anticancer activity was studied against human breast carcinoma (MDA-MB-231), human prostate carcinoma (PPC-1), and human glioblastoma (U-87). Compounds 4, 9, 14, and 22 were identified as the most promising anticancer agents from a series of imidazole derivatives. They showed the highest cytotoxicity by MTT assay against MDA-MB-231, PPC-1 and U-87 cell lines. Compounds 14 and 22 were most selective against PPC-1 and U-87 cell lines, and their EC_{50} values against these cell lines ranged from 3.1 to 47.2 µM. Most tested compounds showed lower activity against the triple-negative breast cancer MDA-MB-231 cell line. None of the imidazole derivatives possessed an inhibiting effect on the migration of PPC-1 and U-87 cells by 'wound' healing assay. In spheroid assay, the most promising were compounds 14 and 22, especially in PPC-1 3D cultures. They efficiently reduced both the size and the viability of PPC-1 spheroid cells.

Keywords Imidazole, Alkylation, Anticancer activity, Cell migration, 3D cell cultures

Although we have entered the 21st century, an era of great scientific, medicinal and technological achievements, cancer still remains an extremely sensitive problem for mankind all over the world. The four most common cancer causes of death in the EU are estimated to be lung (19.5% of all cancer deaths), followed by colorectal (12.3%), breast (7.5%), and pancreatic cancer (7.4%). As the European Cancer Information System (ECIS) report says, new cancer cases rose by 2.3% compared to 2020 and reached 2.74 million in 2022. Similarly, deaths increased by 2.4% compared to 2020[1].

Despite the abundance and availability of anticancer drugs, many cancer forms remain difficult to cure, resulting in growing death rates. Another relevant issue is that the treatment of patients is faced with the increasing resistance of cancer cells to the various anticancer drugs that are currently in use). There is always a constant need for the search of new potent compounds with better safety profiles and novel mechanisms of action, that can overcome the limitation of existing drugs[2].

Imidazole derivatives have great potential to overcome the outstanding shortcomings of currently available therapeutic drugs. They can be used as a chemical basis for new anticancer drugs with several possible mechanisms of action. Unlike other heterocycles, the imidazole core with electron-rich features is a significant medicinal scaffold, which freely binds with protein molecules and various receptors and enzymes in biological systems[3]. Thus, imidazole-based compounds are important in the search for agents to treat cancer, as well as important drugs for therapeutic use. Since 1840, when imidazole was discovered[4], the research and development

[1]Kaunas University of Technology, Radvilėnų Rd. 19, Kaunas LT-50254, Lithuania. [2]Lithuanian University of Health Sciences, A. Mickevičiaus St. 9, Kaunas LT-44307, Lithuania. [3]Institute of Biotechnology, Life Sciences Center, Vilnius University, Saulėtekio Ave. 7, Vilnius LT-10257, Lithuania. ✉email: vytautas.mickevicius@ktu.lt; vilma.petrikaite@lsmuni.lt

of its synthetic derivatives became an active area of investigation[5–8]. In 1975, after the approval of the imidazole derivative dacarbazine as a chemotherapeutic agent (Fig. 1), which is still successfully applied for the treatment of melanoma and Hodgkin's lymphoma[9], imidazole became one of the priority research areas of medicinal chemistry. Currently, many imidazole-based agents, such as ponatinib, fadrozole, temozolomide, nilotinib, azathioprine, bendamustine and tipifarnib (Fig. 1), are tested in clinics as potential anticancer drugs to cure of various types of cancer[10–12].

Various studies have shown that changes in the structure and function of DNA, and profuse receptors and enzymes determine the occurrence of various types of cancer[13]. Therefore, researchers of medicinal chemistry are concerned with discovering, determining and identifying the mechanism of action of biologically active compounds at the molecular level. Many studies published revealed imidazoles to be excellent radiosensitizers, microtubule destabilizing anticancer agents, antiangiogenic, antiproliferative and resistance reversal agents. They also showed potency as enzyme inhibitors[11,13–18]. These discoveries disclose the vital role of various substituted imidazoles in modern drug searches.

For testing the anticancer potential of synthesized imidazole derivatives, we chose human triple-negative breast cancer, primary prostate carcinoma, and glioblastoma cell lines. Triple-negative breast cancer is known as a very aggressive, metastatic, and often recurrent type of breast cancer with a poor prognosis[19]. Due to the lack of estrogen, progesterone, epidermal growth factor (HER-2) receptors, and various molecular subtypes, its treatment options are limited and complicated[20]. Human glioblastoma is considered one of the deadliest human cancers, with the median survival after diagnosis of only 15 months[21]. Usually, this brain cancer is undergoing surgery followed by radiotherapy and chemotherapy, and the available treatment options are very limited[22]. Meanwhile, prostate carcinoma is characterised by relatively slow growth and higher survival, though it is the second most frequent type of cancer in men worldwide[23]. However, despite better prognosis and advanced therapeutic options for this cancer, the metastatic resistant prostate cancer is still considered a deadly disease[24]. Thus, novel treatment strategies are needed, preferably with fewer side effects, greater activity, and potentially lower tendencies of development of cancer resistance.

The aim of our research was to synthesize a library of novel imidazol-2-ones and their thio analogues for the assessment of their activity against the triple-negative breast (MDA-MB-231), human prostate (PPC-1), and human glioblastoma (U-87) cancer cell lines. As the intermediate compounds, aminoethanones were chosen, which were then used for the preparation of ketoxime, oxo- and thioxoimidazoles, and the latter were then treated with alkylating agents to give S-, O-, and N-alkylated derivatives. This choice was based on the fact that chemically derived oximes, as highly biologically active molecules, are widely used in many areas, especially in the medicinal chemistry[25–27], imidazolone- and imidazolethione-type compounds are well known for their anticancer and antitumor properties[28–30], 2-oxo- and 2-thioxoimidazoles with different structures of O- and S-side alkyl chains have interesting and useful biological activities, including anticancer ones[31–33]. In terms of anticancer activity, C=S or NH alkylation of the imidazole ring led to compounds, inhibiting the colony formation of melanoma and triple-negative breast cancer cells and the growth of cancer spheroids[34].

To identify the best candidates from this series of compounds, we decided to screen compounds in all three cell lines by establishing their effect on cell viability, then continue experiments by determining the cell migration inhibition effect, which is related to potential antimetastatic properties relevant to selected types of cancer. Finally, we planned to test the compound activity in cell 3D cultures (cell spheroids) that better resemble the tumour microenvironment by their organizational structure and the gradient of oxygen (hypoxic core) and substances inside (including a gradient of tested materials)[35].

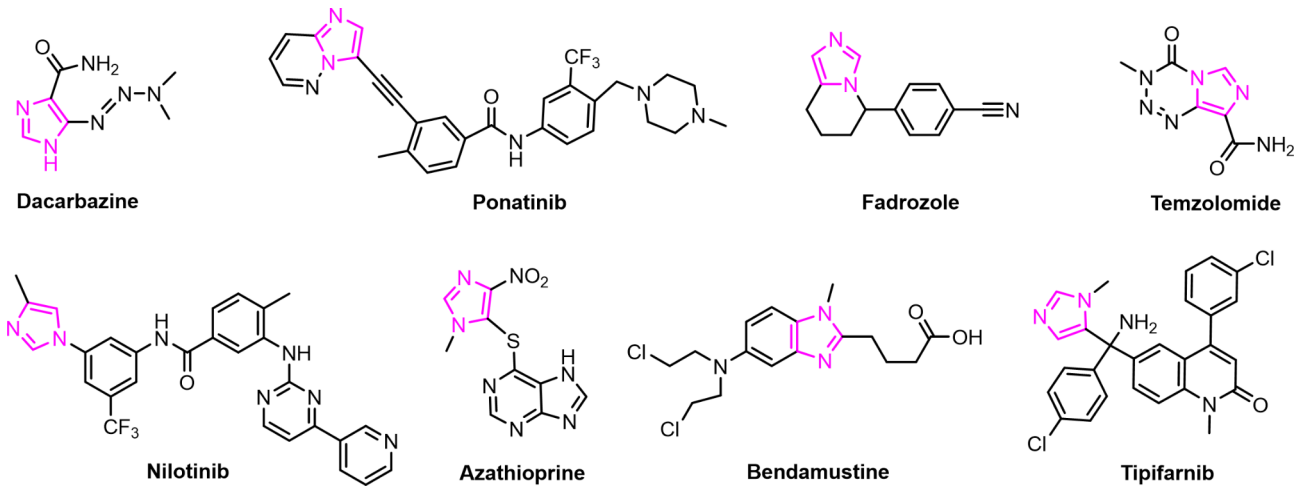

Fig. 1. Some examples of currently tested anticancer agents in clinics.

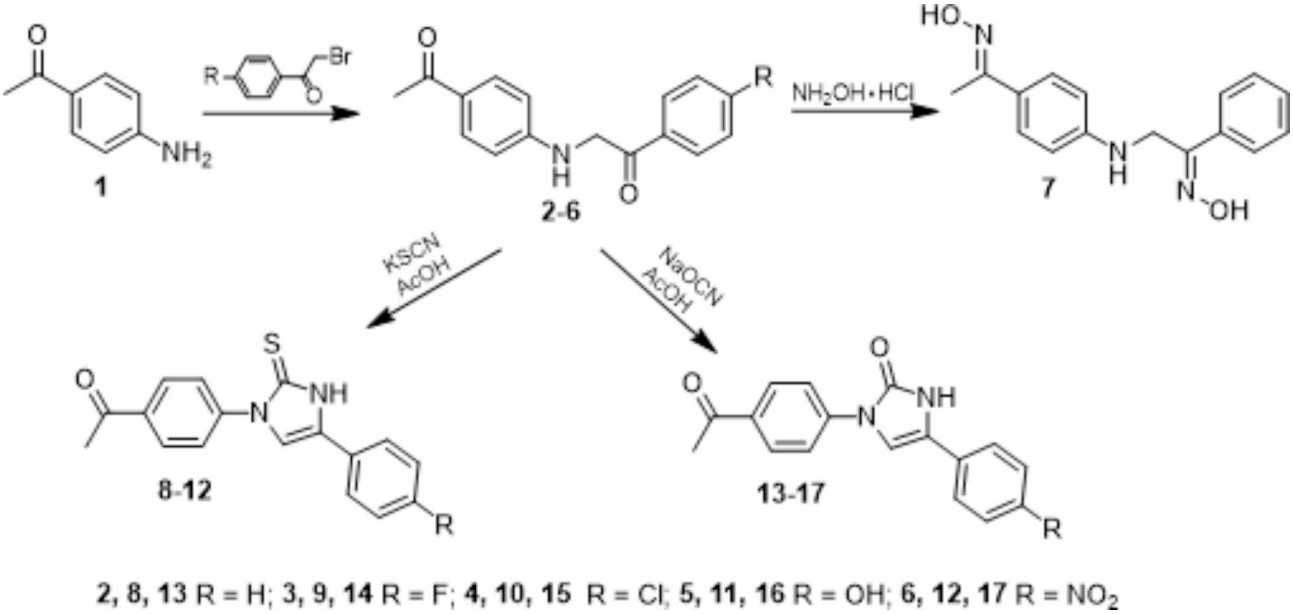

Fig. 2. Synthesis of 2-((4-acetylphenyl)amino)-1-(aryl)ethan-1-ones **2–6** and their modifications.

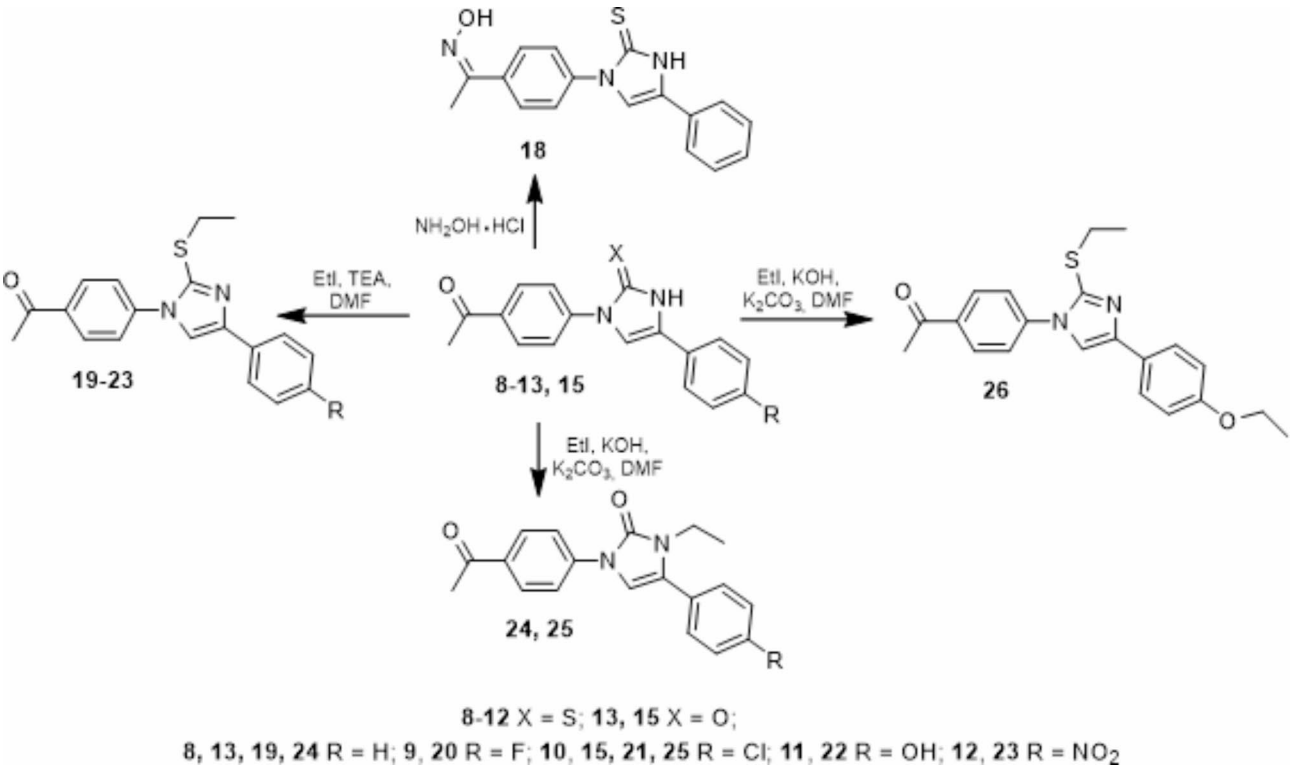

Fig. 3. Some chemical transformations of 1,4-disubstituted imidazoles **8–13**, **15**.

Results and discussion

Chemistry

The strategy to create heterocyclic imidazoles was based on the reactions of 2-((4-acetylphenyl)amino)-1-phenylethan-1-ones with cyanates (Fig. 2) and further derivatization of the resulting products using carbonyl, thiocarbonyl and N-3 positions (Fig. 3) to find compounds with anticancer properties. Initially, 1-(4-aminophenyl)ethan-1-one **(1)** upon reaction with various *α*-haloketones (Fig. 2) in refluxing propan-2-ol–water (1:2) mixture for 3 h resulted in the target 2-((4-acetylphenyl)amino)-1-arylethan-1-ones **2–6** in 85–94%

yield. The formation of the compounds was approved based on their spectral analysis. The ^{1}H NMR spectra revealed the appearance of the $NHCH_2C=O$ protons, and the ^{13}C NMR spectra showed additional resonance lines for carbons of the $NHCH_2C=O$ fragment. The remaining spectral lines were in excellent agreement with the proposed structures (Supplementary Files, Figs S1−S10). The mass spectra of compounds **2–6**, showed the molecular ions M^+ peaks close to the calculated ones.

Afterwards, we exploited the ability of carbonyl compounds to react with hydroxylamine hydrochloride and attempted to synthesize diketoxime **7** using 2-((4-acetylphenyl)amino)-1-phenylethan-1-one **(2)** in the reaction with $NH_4OH{\cdot}HCl$ in the presence of sodium acetate in the mixture. After 2 h of heating at reflux, the oxime **7** was isolated in a high 87% yield. The method used has some advantages: easy reaction conditions, short reaction time of only up to 2 h, no side reactions, and easy separation of the products. The oxime structure was established by IR, NMR and mass spectrometry. The comparison of the ^{1}H and ^{13}C NMR spectra of the starting compound **2** and the obtained oxime **7** revealed obvious differences between them and showed formation of the target product (Supplementary Files, Fig. S11, 12). The mass spectroscopic data approved the desired structure as well.

Noteworthy to mention, that in the case of ketoxime **7**, the mixture of the *E*- and *Z*-isomers with the ratio of 78:22 was observed[36,37]. The isomers were not separated during the research, as we did not set such a task at this initial stage of research.

Knowing the important role of oxo- and thioxoimidazoles, we decided to include their synthesis in the study. Thus, to obtain imidazolethiones **8–12** and their *O*-analogues **13–17**, *α*-amino ketones **2–6** were reacted with potassium thiocyanate or sodium cyanate in refluxing acetic acid for 3–4 h, respectively. The reactions afforded heterocyclic imidazole-2-thione **8–12** or imidazol-2-one derivatives **13–17**. The spectral data fully approved the formation of the desired cycle in the molecular structures 8–**12** (Supplementary Files, Figs S13−22) and **13–17** (Supplementary Files, Figs S23−32).

The next step of the study was chemical transformations of the synthesized imidazole derivatives **8–13**, **15**. Treatment of compound **8** with hydroxylamine hydrochloride gave monoketoxime **18** an excellent 95% yield. Although oximes usually form a mixture of isomers, in this case, the compound was obtained in the form of a single isomer, which is clearly observed in the ^{1}H NMR spectrum of the crude product (Supplementary Files, Figs. S33, S34).

Further, with compounds **8–13**, **15** in the hands, some of their *O*-, *S*- and *N*-modifications were carried out. The reaction of imidazoles **8–12** with ethyl iodide in the presence of a triethylamine base in the reaction mixture in dimethylformamide gave only the *S*-alkylated products **19–23**. When the *S*-alkylation reaction of derivative **11** was repeated by adding ground potassium hydroxide and potassium carbonate to the reaction mixture instead of TEA, alkylation occurred at two positions, resulting in the *S*- and *O*-alkylated compound **26**, which was clearly shown by NMR spectra of the derivative.

When *O*-analogues **13** and **15** were alkylated under the same conditions as for compound **26**, *N*-alkylation occurred, and 3-ethylimidazolin-2-ones **24** and **25** were separated from the reaction mixtures (Supplementary Files, Figs S45−48).

Compound cytotoxicity

The tested imidazole derivatives showed different cytotoxicity against human triple-negative breast cancer (MDA-MB-231), prostate adenocarcinoma (PPC-1) and glioblastoma (U-87) cell lines at 100 μM (Fig. 4). This concentration was used for screening of the most active compounds, based on their solubility and our research experience[38,39].

When analysing the structure-activity relationship (SAR), it is noteworthy to note the influence of the substituents on the phenyl ring on the activity of the compounds. As for compounds **20**, **21** and **22**, the

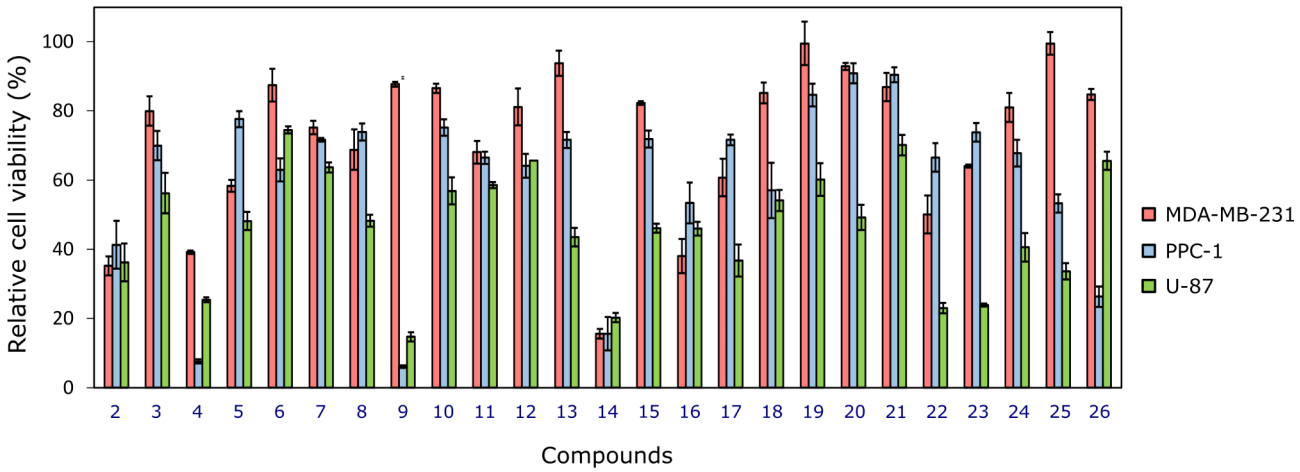

Fig. 4. Effect of imidazole derivatives 1–25 on cancer cell viability at 100 μM concentration against human triple-negative breast cancer MDA-MB-231, prostate cancer PPC-1, and glioblastoma U-87 cell lines. Cytotoxicity was established by the MTT assay after 72 h of incubation with 100 μM of compound solutions, $n = 3$.

incorporation of an electron-donating OH group in the phenyl ring of the S-alkylated molecule **22** increased the biological activity of the compound, while the electron-withdrawing halo substituents F and Cl weakened the activity of the analogues compounds **20** and **21**. Meanwhile, the electron-withdrawing halo substituents (F, Cl) on the phenyl ring in aminoethanone **4**, and non-alkylated imidazolethione **9** or imidazolone **14** positively influence the anticancer potency of the compounds. Again, strong electronegativity and electron-withdrawing properties of the fluorine in imidazolone **14** enhance the activity of the compound compared to the electron-donating hydroxyl group in the analogous compound **16**.

Most of the compounds at 100 µM did not reduce cancer cell viability by more than 50%. Only four compounds – aminoketones **2** and **4** with phenyl and 4-chlorophenyl substituents, imidazole thione **14** with 4-fluorophenyl substituent and oxoimidazole **16** with 4-chlorophenyl substituent reduced MDA-MB-231 cell viability up to 50%. Similarly, five derivatives **2**, **4**, **9**, **14** and **26** (imidazolethione **9** with 4-fluorphenyl substituent and S-ethylthioimidazole **26** with 4-ethoxyphenyl substituent) showed an effect on prostate cancer cell PPC-1, by diminishing their 50% viability. The highest cytotoxicity was established towards human glioblastoma U-87 cells – 15 out of 25 tested compounds reduced 50% of their viability. In total, during preliminary screening, only three compounds (**4**, **9** and **14**) showed effect on more than 80% of cell reduction. These compounds were selected as the most promising testing materials for more detailed studies. Additionally, compound **22** was also chosen due to its expressed selectivity towards U-87 cells.

EC_{50} values were established not only against cancer cells but also human fibroblasts in order to evaluate their selectivity towards cancer (Fig. 5).

It was determined that compounds did not show selectivity for MDA-MB-231 cells. Furthermore, compounds **4** and **9** did not reveal selectivity towards the glioblastoma cell line. The highest selectivity for all four compounds was established against the prostate adenocarcinoma cancer cell line. They showed higher activity towards PPC-1 cell lines compared to fibroblasts from 1.7 (compound **22**) to 14.5 times (compound **14**). Compounds **14** and **22** were determined as the best candidates against PPC-1 and U-87 cancer cells, especially compound **14**. The EC_{50} values for this compound were 4.1 ± 1.0 µM against PPC-1 cell line, and 3.1 ± 0.1 µM against U-87 cell line.

Relatively low activity against human triple-negative breast cancer MDA-MB-231 cell lines could be explained by its known aggressiveness and low response to many chemotherapeutic drugs. Already during its establishment, it was noted that this cell line grows fast and vigorously and forms tumor nodules in nude mice in 6 weeks after injection[40]. The mechanisms responsible for its resistance are still extensively studied[41], while at the same time, it is recognised that triple-negative breast cancer is a very heterogeneous disease, and finding therapeutics for this type of cancer is challenging[42]. However, the activity of small synthetic molecules from different classes varies a lot between them and also between different types of breast cancer cells, showing EC_{50} values ranging from nanomolar concentration to several tens of micromolars[43]. Interestingly, the compound from the 6, N2-diaryl-1,3,5-triazine-2,4-diamine derivatives showed activity against MDA-MB-231 cell lines with EC_{50} of 1 nM without cytotoxicity against the normal cell of MCF-10 A breast[44]. In this study, the 4-acetylphenylamine-based imidazole derivatives were not very active nor selective towards used breast cancer cell lines; thus, we decided not to test compounds in another two-dimensional assay for cell migration, and only to compare their activity in 3D cultures, considering different cell-cell interactions, gene expression, nutrient and oxygen gradient in this model[25].

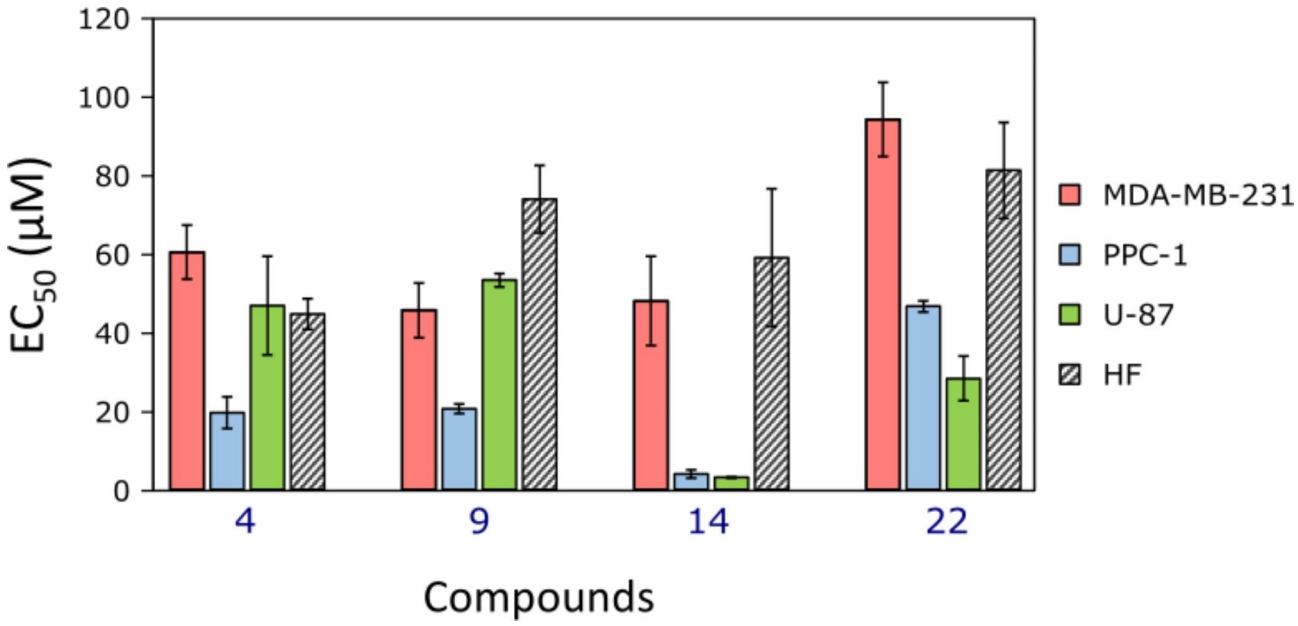

Fig. 5. EC_{50} values of the most active compounds **4**, **9**, **14** and **22** by MTT assay, after 72 h of incubation. $n = 3$. EC_{50} values were calculated from the dose-response curves using the Hill equation.

The effect of compounds on glioblastoma U-87 cell line viability varied in a micromolar range from 3.1 to 53.9 μM (Fig. 5), suggesting a hypothesis that tested compounds could possess different pharmacokinetic properties and mechanisms of action. U-87 cell line is usually resistant to many chemical agents, and it is explained partly by the stem cell population presence in it[45]. However, one of the most often used anti-glioblastoma drug temozolomide reduced U-87 cell line viability only at 86.21 ± 23.8 μM, by the same method after 72 h of incubation, and this activity is comparable with the other studies[46]. The activity and selectivity of compounds **14** and **22** against the glioblastoma cell line seem promising and encouraged us to continue experiments in this cell line.

The cytotoxic effect in prostate carcinoma PPC-1 cell lines was moderate compared to the other two cell lines (Fig. 4). This cell line is characterized by tumorigenic properties in nude mice and also metastatic potential[47]. However, the established activity in PPC-1 for most compounds (EC_{50} values were from 4.1 to 47.2 μM) was higher compared to the anticancer alkylating drug cisplatin effect in this cell line (EC_{50} = 27.8 ± 11.1 μM). On the other hand, all four compounds were less active compared to other anticancer drugs paclitaxel, gemcitabine and 5-fluorouracil (EC_{50} = 1.3 ± 0.4 nM, 43.0 ± 15.4 nM and 1.7 ± 0.3 μM, respectively). Considering the need for this widely spread type of cancer and established activity comparable to anticancer agents, further studies on cell migration were performed.

Compound effect on cell migration

Considering the results from cytotoxicity, as discussed above, we decided to test the compound effect on PPC-1 and U-87 cell migration. To avoid or at least diminish the effects related to cytotoxicity and to equalise the cytotoxic effect for all compounds, we used 50% of established EC_{50} for each individual compound. Glioblastoma U-87 cells migrated faster than PPC-1 cells, and the 'wound' area closed already 24 h after the beginning of the experiment (Fig. 6). Thus, the photos for this cell line were taken only after 12 and 24 h. Meanwhile, the 'wound' in the PPC-1 cell monolayer in the control group 'healed' slowly, and the images of the 'wound' area were taken at three time points (24, 48, and 72 h) from the beginning of the scratch.

Overall, the effect of imidazole derivatives on cell migration inhibition was low. Despite some slight effects of compounds **9**, **14**, and **22** on U-87 cell migration after 24 h of incubation, none of the four tested compounds showed a statistically significant effect on cancer cell migration (Fig. 6). Considering that the concentrations of the used compounds were relatively high, and the effect was not established, we concluded that tested imidazole derivatives do not possess the inhibiting effect on both U-87 and PPC-1 cell migration.

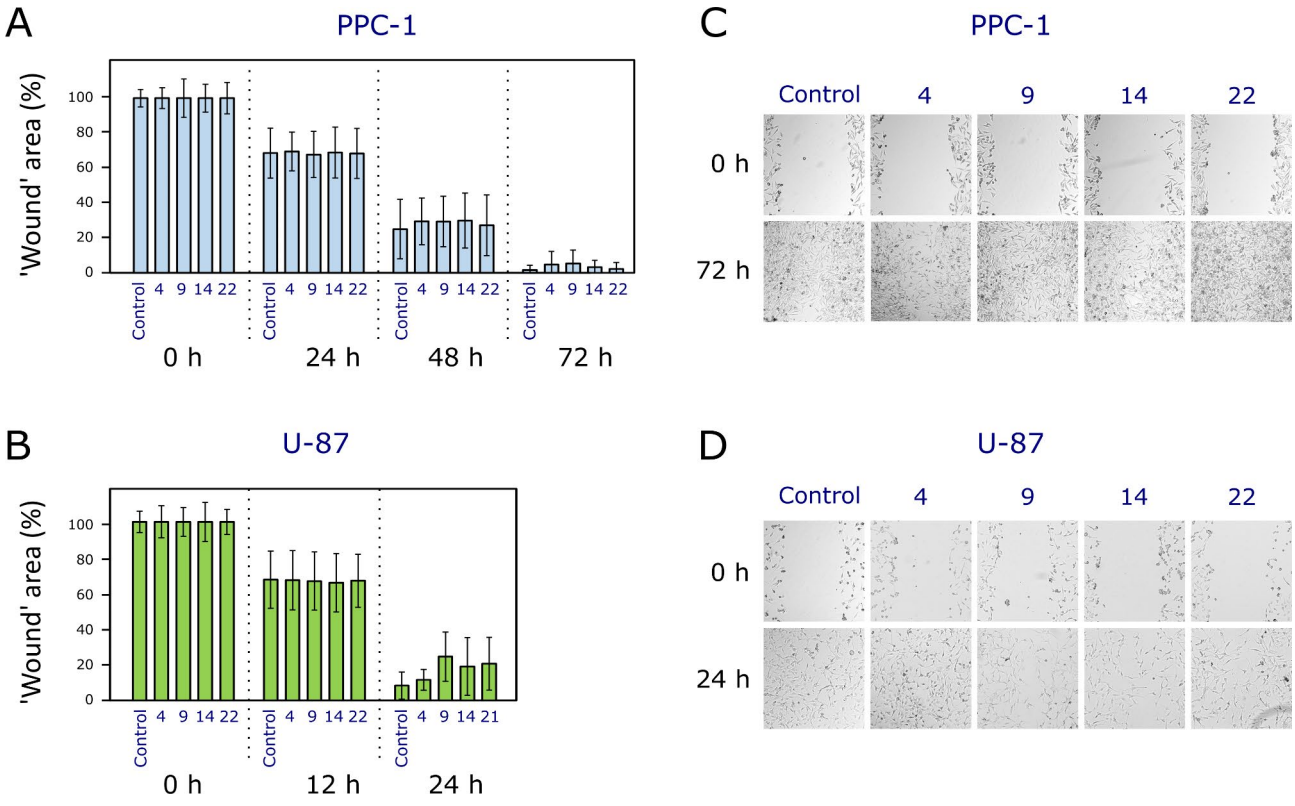

Fig. 6. Effect of compounds **4**, **9**, **14**, and **22** on human prostate adenocarcinoma PPC-1 (**A**) and human glioblastoma U-87 (**B**), cell migration, $n = 3$. Photos of the 'wound' area in PPC-1 (**C**) and U-87 (**D**) monolayer at the beginning and the end of the experiment.

Compound effect in three-dimensional cell cultures (spheroids)

Spheroids were made of cancer cells combined with fibroblasts at a ratio of 1:1 to better represent the real tumour microenvironment. Fibroblasts serve as stroma cells and help to maintain a three-dimensional structure, providing an extracellular matrix, which contributes to making this model more representative of the in vivo tumour situation[48].

At the beginning of the experiment, all types of spheroids were about 300 µm in diameter (Fig. 7D, E and **F**). However, MDA-MB-231 spheroids were faster up to day 4, but later, they became irregular in shape, and the cells from the outer layers started to even break away from the spheroids (Fig. 7A). The U-87 spheroids grew slower but constantly over the whole experiment duration and retained a more oval shape (Fig. 7C). Meanwhile, the PPC-1 spheroids were characterized by the most irregular shape and most loose at the end of the experiment (Fig. 7B). Spheroid growth was affected differently by tested compounds. However, similar trends were established in all

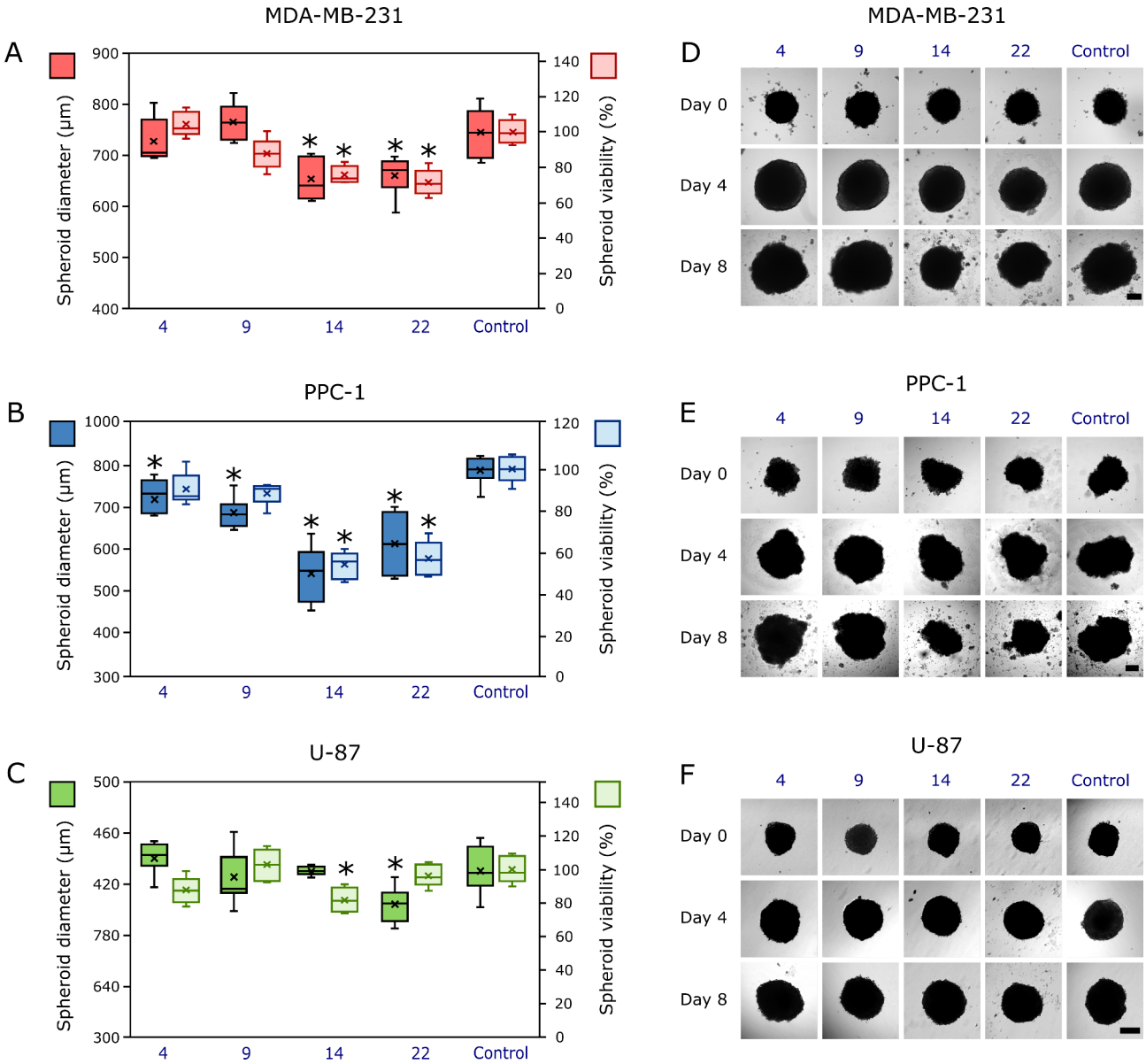

Fig. 7. Effect of compounds **4**, **9**, **14**, and **22** at 10 µM concentration on 3D cell cultures. (**A**) Size and viability of human triple-negative breast cancer MDA-MB-231 tumour spheroids at the end of experiment (after 8 days of incubation). (**B**) Size and viability of human prostate carcinoma PPC-1 tumour spheroids at the end of experiment (after 8 days of incubation). (**C**) Size and viability of human glioblastoma U-87 tumour spheroids at the end of experiment (after 8 days of incubation). (**D**) Photos of human triple-negative breast cancer MDA-MB-231 tumour spheroids. (**E**) Photos of human prostate carcinoma PPC-1 tumour spheroids. (**F**) Photos of human glioblastoma U-87 tumour spheroids. The spheroid number per group was 6–8. Asterisks (*) indicate $p < 0.05$ compared to the control (untreated spheroids); crosses (×) indicate means; inner dashes indicate medians, and whiskers indicate maximum and minimum values. Scale bars indicate 200 µm.

cases: compounds **14** and **22** were the most active and showed the highest effect on cell spheroid size/viability (Fig. 7A, B, C). Compounds **4** and **9** affected the growth of only PPC-1 spheroids, but they did not reduce the cell viability. On the contrary, the U-87 spheroids incubated with compound **14** were of the same size as the control group; still, their viability was lower (Fig. 7B). Compound **22** inhibited the growth of all spheroids but did not affect the viability of U-87 spheroids (Fig. 7C) ($p > 0.05$). Generally, the most active was compound **14**, which reduced the PPC-1 spheroid cell viability by up to 54.5 ± 6.7%. It is generally known that the MTT assay has some limitations, including the reagent penetration into the deeper layers of spheroids; however, it is still used quite often by many scientists for measuring compound and nanoparticle effects on cell viability inside the 3D cell cultures[49,50]. In our research, we included both positive and negative controls, which were used to test the validity of the developed experimental methodologies. Taking into consideration the limitations of the MTT assay and spheroid size/morphology observation alone, we combined those two different approaches, and we believe that this combination helps better understand the compound effects in these cultures.

The variability of compound effect on spheroid size and their viability was already established by many scientists and by us[39,51,52]. Thus, we measure those two parameters in parallel to make more accurate conclusions on the compound effect in cell 3D cultures. In this study, the effect of tested imidazole derivatives on MDA-MB-231 and U-87 spheroid viability was relatively lower compared to the PPC-1 spheroids, which aligns with the obtained cytotoxic activity results in these cell lines and could be explained by their higher innate aggressiveness as already discussed. The differences between compound activity in 3D cultures were not so great as established in a cell monolayer, and one could hypothesise that specific factors that are relevant to spatial cell architecture and other related properties could contribute to it[48]. Considering that the spheroid model better represents the in vivo situation, we suggest that compounds **14** and **22** could be worthy of more detailed studies, especially in the prostate cancer model, including establishing their mechanism of action.

However, it should also be noted that the studies in spheroids grown in plastic plates (as it is in this case) bring us to a slightly advanced level of studying the compound effect in 3D cultures, but they lack the complexity of interactions that occur in vivo due to the absence of an extracellular matrix (ECM)[53]. The 3D cultures with ECM scaffolds would offer a more representative environment for modelling tissue behaviour, cellular differentiation, invasion, and response to compound treatments[54], however, in our studies for convenience, we chose the more simplified method for making spheroids simultaneously of a very similar size, which was more practical for the primary screening[55].

However, we agree with the limitations of our study regarding establishing the biological target. It is known that different classes of imidazole derivatives are targeting different pathways in cancer cells. A group of imidazothiazoles were identified as potent and selective ErbB4 (HER4) inhibitors[56]. Imidazole derivatives possessing terminal sulphonamides with the inhibition potential of BRAF kinase, showed relatively strong cytotoxicity against melanoma cancer cells[57]. Different mechanisms of action of various imidazole derivatives were reviewed by Sharma et al., and the possible targets include microtubules, tyrosine and serine-threonine kinases, MDM2 protein, PARP, etc[18]. Considering such variety of potential targets, in our study first we aimed to identify the most active compounds in different assays, and determine the candidates for further target prediction and validation, as well as molecular docking studies.

Conclusions

In this study, a series of S- and N-substituted imidazoles with aliphatic, aromatic fragments were synthesized and evaluated for their anticancer activities. In biological assays, 2-((4-acetylphenyl)amino)-1-(4-chlorophenyl) ethan-1-one **(4)**, 1-(4-(4-(4-fluorophenyl)-2-thioxo-2,3-dihydro-1*H*-imidazol-1-yl)phenyl)ethan-1-one **(9)**, 1-(4-acetylphenyl)-4-(4-fluorophenyl)-1,3-dihydro-2*H*-imidazol-2-one **(14)**, and 1-(4-(2-(ethylthio)-4-(4-hydroxyphenyl)-1*H*-imidazol-1-yl)phenyl)ethan-1-one **(22)** were identified as the most promising anticancer agents out of a series of imidazole derivatives. They showed the highest cytotoxicity against triple-negative breast cancer MDA-MB-231, prostate carcinoma PPC-1 and glioblastoma U-87 cell line. Compounds **14** and **22** were most selective against PPC-1 and U-87 cell lines, and their EC_{50} values against these cell lines ranged from 3.1 to 47.2 µM. Most tested compounds showed lower activity against the triple-negative breast cancer MDA-MB-231 cell line. None of the imidazole derivatives possessed an inhibiting effect on the migration of PPC-1 and U-87 cells. In spheroid assay, the most promising were compounds **14** and **22**, especially in PPC-1 3D cultures. They efficiently reduced both the size and the viability of PPC-1 spheroid cells.

Materials and methods

General procedures

Reagents and solvents were purchased from Sigma-Aldrich (St. Louis, MO, USA) and used without further purification. The reaction course and purity of the synthesized compounds were monitored by TLC using aluminium plates pre-coated with Silica gel with F_{254} nm (Merck KGaA, Darmstadt, Germany). Melting points were determined with a *B-540* melting point analyser (Büchi Corporation, New Castle, DE, USA) and were uncorrected. IR spectra (ν, cm^{-1}) were recorded on a Perkin–Elmer Spectrum BX FT–IR spectrometer (Perkin–Elmer Inc., Waltham, MA, USA) using KBr pellets. NMR spectra were recorded on a Brucker Avance III (400, 101 MHz) spectrometer (Bruker BioSpin AG, Fällanden, Switzerland). Chemical shifts were reported in (δ) ppm relative to tetramethylsilane (TMS), with the residual solvent as internal reference (DMSO-d_6, $\delta = 2.50$ ppm for ^{1}H and $\delta = 39.52$ ppm for ^{13}C). Data are reported as follows: chemical shift, multiplicity, integration, coupling constant [Hz], and assignment. Mass spectra were obtained on a maXis UHR-TOF mass spectrometer (Bruker Daltonics, Bremen, Germany) with ESI ionization. Elemental analysis (C, H, N) was conducted on an Elemental Analyzer CE-440 (Exeter Analytical, Inc., Chelmsford, MA, USA), and the results were found to be in good agreement (± 0.3%) with the calculated values.

Synthetic procedures

General procedure for the synthesis of 2–6.

4′-Aminoacetophenone (**1**) (10 g, 74 mmol) was dissolved in boiling propan-2-ol (80 mL) and water (160 mL) mixture. Then corresponding α-haloketone (89 mmol) was added, and the reaction mixture was heated at reflux for 3 h, then cooled, and the precipitate was filtered off, washed with propan-2-ol, and recrystallized to afford compounds **2–6**.

2-((4-Acetylphenyl)amino)-1-phenylethan-1-one (2)

White solid, yield 16.17 g (86%); m.p. 198–199 °C (propan-2-ol);

IR (KBr) (ν, cm^{-1}): 1663, 1689 (2 C=O), 3359 (NH);

^{1}H NMR (400 MHz, DMSO-d_6) δ (ppm): 2.40 (s, 3 H, CH_3), 4.81 (d, 2 H, J=5.4 Hz, CH_2), 6.72 (d, 2 H, J=8.6 Hz, H_{Ar}), 6.81 (t, 1H, J=5.3 Hz, NH), 7.57 (t, 2 H, J=7.6 Hz, H_{Ar}), 7.68 (d, 1H, J=7.3 Hz, H_{Ar}), 7.72 (d, 2 H, J=8.7 Hz, H_{Ar}), 8.08 (d, 2 H, J=7.7 Hz, H_{Ar});

^{13}C NMR (101 MHz, DMSO-d_6) δ (ppm): 25.95 (CH_3), 49.34 (CH_2), 111.45, 125.39, 127.96, 128.84, 130.29, 133.69, 134.97, 152.47 (C_{Ar}), 195.19 (CH_2C=O), 195.95 (CH_3C=O);

HRMS (ESI): *m/z* calcd. for $C_{16}H_{16}NO_2$ 254.1181; found: 254.1174 $[M+H]^+$.

2-((4-Acetylphenyl)amino)-1-(4-fluorophenyl)ethan-1-one (3)

White solid, yield 18.61 g (93%); m.p. 209–210 °C (propan-2-ol);

IR (KBr) (ν, cm^{-1}): 1599, 1690 (2 C=O), 3359 (NH);

^{1}H NMR (400 MHz, DMSO-d_6) δ (ppm): 2.40 (s, 3 H, CH_3), 4.80 (d, 2 H, J=5.4 Hz, CH_2), 6.71 (d, 2 H, J=8.5 Hz, H_{Ar}), 6.81 (t, 1H, J=5.3 Hz, NH), 7.41 (t, 2 H, J=8.6 Hz, H_{Ar}), 7.72 (d, 2 H, J=8.4 Hz, H_{Ar}), 8.16 (dd, 2 H, J=8.0, 5.8 Hz, H_{Ar});

^{13}C NMR (101 MHz, DMSO-d_6) δ (ppm): 25.94 (CH_3), 49.31 (CH_2), 111.44, 115.86 (d, J=22 Hz), 125.41, 130.27, 130.32, 131.02 (d, J=9.6 Hz), 152.44, 167.22 (d, J=243.6 Hz) (C_{Ar}), 194.62 (CH_2C=O), 195.17 (CH_3C=O);

HRMS (ESI): *m/z* calcd. for $C_{16}H_{15}FNO_2$ 272.1087; found: 272.1080 $[M+H]^+$.

2-((4-Acetylphenyl)amino)-1-(4-chlorophenyl)ethan-1-one (4)

Yellow solid, yield 20.02 g (94%); m.p. 182–183 °C (propan-2-ol);

IR (KBr) (ν, cm^{-1}): 1653, 1687 (2 C=O), 3385 (NH);

^{1}H NMR (400 MHz, DMSO-d_6) δ (ppm): 2.40 (s, 3 H, CH_3), 4.80 (d, 2 H, J=5.4 Hz, CH_2), 6.71 (d, 2 H, J=8.5 Hz, H_{Ar}), 6.81 (t, 1H, J=5.3 Hz, NH), 7.65 (d, 2 H, J=8.3 Hz, H_{Ar}), 7.72 (d, 2 H, J=8.5 Hz, H_{Ar}), 8.09 (d, 2 H, J=8.3 Hz, H_{Ar});

^{13}C NMR (101 MHz, DMSO-d_6) δ (ppm): 25.94 (CH_3), 49.40 (CH_2), 111.45, 125.43, 128.93, 129.91, 130.27, 133.65, 138.54, 152.41 (C_{Ar}), 195.11 (CH_2C=O), 195.18 (CH_3C=O);

HRMS (ESI): *m/z* calcd. for $C_{16}H_{15}ClNO_2$ 288.0791; found: 288.0782 $[M+H]^+$.

2-((4-Acetylphenyl)amino)-1-(4-hydroxyphenyl)ethan-1-one (5)

Yellow solid, yield 17.37 g (85%); m.p. 196–197 °C (propan-2-ol);

IR (KBr) (ν, cm^{-1}): 1600, 1659 (2 C=O), 3143 (OH), 3371 (NH);

^{1}H NMR (400 MHz, DMSO-d_6) δ (ppm): 2.40 (s, 3 H, CH_3), 4.68, 4.73 (2s, 2 H, CH_2), 6.70 (d, 2 H, J=8.4 Hz, H_{Ar}), 6.89 (d, 2 H, J=8.2 Hz, H_{Ar}), 6.90, 7.09 (2t. 1H, J=7.0 Hz, NH), 7.72 (d, 2 H, J=8.4 Hz, H_{Ar}), 7.96, 8.03 (2d, 2 H, J=8.3 Hz, H_{Ar}), 10.45, 10.51 (2s, 1H, OH);

^{13}C NMR (101 MHz, DMSO-d_6) δ (ppm): 25.51, 25.94 (CH_3), 48.75, 48.95 (CH_2), 111.43, 114.67, 115.36, 115.43, 125.30, 126.49, 130.16, 130.29, 130.53, 152.49, 162.48, 162.70 (C_{Ar}), 193.75 (CH_2C=O), 195.15 (CH_3C=O);

HRMS (ESI): *m/z* calcd. for $C_{16}H_{16}NO_3$ 270.1130; found: 270.1123 $[M+H]^+$.

2-((4-Acetylphenyl)amino)-1-(4-nitrophenyl)ethan-1-one (6)

Orange solid, yield 20.62 g (93%); m.p. 183–184 °C (DMF);

IR (KBr) (ν, cm^{-1}): 1653, 1690 (2 C=O), 3384 (NH);

^{1}H NMR (400 MHz, DMSO-d_6) δ (ppm): 2.41 (s, 3 H, CH_3), 4.89 (d, 2 H, J=1.8 Hz, CH_2), 6.73 (d, 2 H, J=8.6 Hz, H_{Ar}), 6.87 (br.s, 1H, NH), 7.73 (d, 2 H, J=8.6 Hz, H_{Ar}), 8.30 (d, 2 H, J=8.6 Hz, H_{Ar}), 8.38 (d, 2 H, J=8.6 Hz, H_{Ar});

^{13}C NMR (101 MHz, DMSO-d_6) δ (ppm): 25.95 (CH_3), 49.95 (CH_2), 111.48, 123.88, 125.54, 129.45, 130.28, 139.64, 150.17, 152.34 (C_{Ar}), 195.21 (CH_2C=O), 195.50 (CH_3C=O);

Calcd. for $C_{16}H_{15}N_2O_4$, %: C 64.21; H 5.05; N 9.36. Found, %: C 64.13; H 5.04; N 9.39.

2-((4-((1-(Hydroxyimino)ethyl)phenyl)amino)-1-phenylethan-1-one oxime (7)

A mixture of compound **2** (2 mmol), hydroxylamine hydrochloride (0.55 g, 7.9 mmol), and sodium acetate (0.65 g, 7.9 mmol) were heated at reflux in propan-2-ol (5 mL) for 2 h. Then volatile fractions were separated under reduced pressure and obtained residue was diluted with water. The obtained crystals were filtered off, washed with water, and recrystallized from 2-propanol.

Brown solid, yield 0.49 g (87%); m.p. 65–66 °C (propan-2-ol);

IR (KBr) (ν, cm^{-1}): 2866, 3057 (2OH), 3214 (NH);

^{1}H NMR (400 MHz, DMSO-d_6) δ (ppm): 2.03, 2.05 (2s, 3 H, CH_3), 4.13, 4.39 (2d, 2 H, J = 5.5 Hz, CH_2), 6.15 (dd, 1H, J = 10.9, 5.3 Hz, NH), 6.55 (d, 1H, J = 7.8 Hz, H_{Ar}), 6.62 (d, 1H, J = 7.9 Hz, H_{Ar}), 7.32–7.47 (m, 5 H, H_{Ar}), 7.52–7.69 (m, 2 H, H_{Ar}) 10.64, 10.65, 10.92, 11.61 (4s, 2 H, 2OH);

^{13}C NMR (101 MHz, DMSO-d_6) δ (ppm): 11.27 (CH_3), 36.40 (CH_2), 111.24, 111.77, 126.39, 126.51, 128.13, 128.27, 128.54, 135.08, 148.70, 149.03, 152.71 (C_{Ar}), 154.97 (C=NOH), 167.75 (C=NOH);

HRMS (ESI): *m/z* calcd. for $C_{16}H_{18}N_3O_2$ 284.1399; found: 284.1392 $[M+H]^+$.

General procedure for the synthesis of 8–12.

To a solution of the corresponding compound **2–6** (20 mmol) in glacial acetic acid (10 mL) KSCN (2.33 g, 24 mmol) was added and the reaction mixture was stirred at reflux for 3 h. Then it was cooled and diluted with water. The obtained crystals were filtered off and washed with water and propan-2-ol to give the title compounds **8–12**.

1-(4-(4-Phenyl-2-thioxo-2,3-dihydro-1*H*-imidazol-1-yl)phenyl)ethan-1-one (8)

White solid, yield 3.82 g (65%); m.p. 268–269 °C (propan-2-ol);

IR (KBr) (ν, cm^{-1}): 1259 (C=S), 1683 (C=O), 3046 (NH);

^{1}H NMR (400 MHz, DMSO-d_6) δ (ppm): 2.64 (s, 3 H, CH_3), 7.33 (t, 1H, J = 7.3 Hz, H_{Ar}), 7.44 (d, 2 H, J = 7.6 Hz, H_{Ar}), 7.78 (d, 2 H, J = 7.6 Hz, H_{Ar}), 7.95 (d, 3 H, J = 7.8 Hz, H_{Ar}, CH), 8.10 (d, 2 H, J = 8.4 Hz, H_{Ar}), 13.08 (s, 1H, NH);

^{13}C NMR (101 MHz, DMSO-d_6) δ (ppm): 26.87 (CH_3), 115.51 (CH), 124.34 (CN), 125.57, 127.55, 128.03, 128.80, 128.94, 135.62, 141.37 (C_{Ar}), 162.80 (C=S), 197.14 (C=O);

HRMS (ESI): *m/z* calcd. for $C_{17}H_{15}N_2OS$ 295.0905; found: 295.0898 $[M+H]^+$.

1-(4-(4-(4-Fluorophenyl)-2-thioxo-2,3-dihydro-1*H*-imidazol-1-yl)phenyl)ethan-1-one (9)

Yellow solid, yield 4.39 g (70%); m.p. 289–290 °C (propan-2-ol);

IR (KBr) (ν, cm^{-1}): 1236 (C=S), 1681 (C=O), 3053 (NH);

^{1}H NMR (400 MHz, DMSO-d_6) δ (ppm): 2.64 (s, 3 H, CH_3), 7.30 (t, 2 H, J = 8.6 Hz, H_{Ar}), 7.86–7.77 (m, 2 H, H_{Ar}), 7.94 (d, 3 H, J = 7.7 Hz, CH, H_{Ar}), 8.10 (d, 2 H, J = 8.2 Hz, H_{Ar}), 8.10 (d, 2 H, J = 8.6 Hz, H_{Ar}), 13.08 (s, 1H, NH);

^{13}C NMR (101 MHz, DMSO-d_6) δ (ppm): 26.88 (CH_3), 115.43, 115.97 (d, J = 21.8 Hz), 124.20 (d, J = 3.0 Hz), 126.54 (d, J = 8.1 Hz), 127.91, 128.82, 135.62, 141.33, 161.72 (d, J = 245.6 Hz) (C_{Ar}), 162.78 (C=S), 197.14 (C=O);

HRMS (ESI): *m/z* calcd. for $C_{17}H_{14}FN_2OS$ 313.0811; found: 313.0803 $[M+H]^+$.

1-(4-(4-(4-Chlorophenyl)-2-thioxo-2,3-dihydro-1*H*-imidazol-1-yl)phenyl)ethan-1-one (10)

Light yellow solid, yield 5.79 g (88%); m.p. 321–322 °C (propan-2-ol);

IR (KBr) (ν, cm^{-1}): 1258 (C=S), 1679 (C=O), 3142 (NH);

^{1}H NMR (400 MHz, DMSO-d_6) δ (ppm): 2.63 (s, 3 H, CH_3), 7.51 (d, 2 H, J = 8.4 Hz, H_{Ar}), 7.79 (d, 2 H, J = 8.4 Hz, H_{Ar}), 7.93 (d, 2 H, J = 8.3 Hz, H_{Ar}), 8.01 (s, 1H, CH), 8.10 (d, 2 H, J = 8.4 Hz, H_{Ar}), 13.12 (s, 1H, NH);

^{13}C NMR (101 MHz, DMSO-d_6) δ (ppm): 26.87 (CH_3), 116.13, 125.55, 126.03, 126.49, 127.68, 128.81, 128.99, 132.42, 135.67, 141.27 (C_{Ar}), 163.01 (C=S), 197.12 (C=O);

HRMS (ESI): *m/z* calcd. for $C_{17}H_{14}ClN_2OS$ 329.0515; found: 329.0500 $[M+H]^+$.

1-(4-(4-(4-Hydroxyphenyl)-2-thioxo-2,3-dihydro-1*H*-imidazol-1-yl)phenyl)ethan-1-one (11)

Yellow solid, yield 4.59 g (78%); m.p. 285–286 °C (propan-2-ol);

IR (KBr) (ν, cm^{-1}): 1265 (C=S), 1668 (C=O) 3175 (OH), 3389 (NH);

^{1}H NMR (400 MHz, DMSO-d_6) δ (ppm): 2.63 (s, 3 H, CH_3), 6.81 (d, 2 H, J = 8.6 Hz, H_{Ar}), 7.58 (d, 2 H, J = 8.6 Hz, H_{Ar}), 7.72 (d, 1H, J = 2.0 Hz, CH), 7.94 (d, 2 H, J = 8.5 Hz, H_{Ar}), 8.09 (d, 2 H, J = 8.6 Hz, H_{Ar}), 9.71 (s, 1H, OH), 12.88 (s, 1H, NH);

^{13}C NMR (101 MHz, DMSO-d_6) δ (ppm): 26.87 (CH_3), 113.43, 115.66, 118.51, 125.42, 126.04, 128.78, 129.28, 135.46, 141.53, 157.50 (C_{Ar}), 162.12 (C=S), 197.14 (C=O);

HRMS (ESI): *m/z* calcd. for $C_{17}H_{15}N_2O_2S$ 311.0854; found: 311.0844 $[M+H]^+$.

1-(4-(4-(4-Nitrophenyl)-2-thioxo-2,3-dihydro-1*H*-imidazol-1-yl)phenyl)ethan-1-one (12)

GB-20 (**12**). Orange solid, yield 5.85 g (86%); m.p. 277–278 °C (DMF);

IR (KBr) (ν, cm^{-1}): 1265 (C=S), 1679 (C=O), 3134 (NH);

^{1}H NMR (400 MHz, DMSO-d_6) δ (ppm): 2.64 (s, 3 H, CH_3), 7.94 (d, 2 H, J = 8.4 Hz, H_{Ar}), 8.03 (d, 2 H, J = 8.8 Hz, H_{Ar}), 8.12 (d, 2 H, J = 8.5 Hz, H_{Ar}), 8.30 (d, 3 H, J = 7.6 Hz, H_{Ar}, CH), 13.35 (s, 1H, NH);

^{13}C NMR (101 MHz, DMSO-d_6) δ (ppm): 26.90 (CH_3), 119.06, 124.39, 124.91, 125.74, 126.80, 128.86, 133.84, 135.92, 141.02, 146.19 (C_{Ar}), 163.96 (C=S), 197.17 (C=O);

Calcd. for $C_{17}H_{14}N_3O_3S$, %: C 59.99; H 4.15; N 12.35. Found, %: C 60.06; H 4.17; N 12.34.

General procedure for the synthesis of 13–17.

To a solution of the corresponding compound **2–6** (20 mmol) in glacial acetic acid (10 mL) sodium cyanate (5.2 g, 80 mmol) was added and the reaction mixture was stirred at reflux for 4 h. Then it was cooled and

diluted with water. The obtained crystals were filtered off and washed with water and propan-2-ol to give the title compounds **13–17**.

1-(4-Acetylphenyl)-4-phenyl-1,3-dihydro-2*H*-imidazol-2-one (13)

Light green solid, yield 4.51 g (81%); m.p. 259–260 °C (propan-2-ol);

IR (KBr) (ν, cm^{-1}): 1693, 1666 (2 C=O), 3053 (NH);

^{1}H NMR (400 MHz, DMSO-d_6) δ (ppm): 2.59 (s, 3 H, CH_3), 7.28 (t, 1H, J=7.3 Hz, H_{Ar}), 7.41 (t, 2 H, J=7.5 Hz, H_{ar}), 7.67 (d, 2 H, J=7.7 Hz, H_{Ar}), 7.78 (s, 1H, CH), 7.99–8.09 (m, 4 H, H_{Ar}), 11.23 (s, 1H, NH);

^{13}C NMR (101 MHz, DMSO-d_6) δ (ppm): 26.62 (CH_3), 106.00, 119.21, 123.18, 123.51, 127.37, 128.76, 128.81, 129.47, 132.92, 141.10 (C_{Ar}), 152.39 (NC=O), 196.75 (CH_3C=*O*);

HRMS (ESI): *m/z* calcd. for $C_{17}H_{15}N_2O_2$ 279.1133; found: 279.1125 $[M+H]^+$.

1-(4-Acetylphenyl)-4-(4-fluorophenyl)-1,3-dihydro-2*H*-imidazol-2-one (14)

White solid, yield 3.42 g (87%); m.p. 162–163 °C (propan-2-ol);

IR (KBr) (ν, cm^{-1}): 1695, 1771 (2 C=O) 3313 (NH);

^{1}H NMR (400 MHz, DMSO-d_6) δ (ppm): 2.59 (s, 3 H, CH_3), 7.28 (t, 3 H, J=8.8 Hz, H_{Ar}), 7.71 (dd, 2 H, J=8.3, 5.6 Hz, H_{Ar}), 7.77 (s, 1H, CH), 8.04 (q, 4 H, J=8.9 Hz, H_{Ar}), 11.24 (s, 1H, NH);

^{13}C NMR (101 MHz, DMSO-d_6) δ (ppm): 26.63 (CH_3), 105.89, 115.84 (d, J=22.1 Hz), 119.17, 122.36, 125.57 (d, J=8.3 Hz), 129.48, 132.94, 141.07, 162.28 (d, J=253.5 Hz) (C_{Ar}), 152.35 (NC=O), 196.76 (CH_3C=*O*);

Calcd. for $C_{17}H_{14}FN_2O_2$, %: C 68.68; H 4.75; N 9.42. Found, %: C 68.52; H 4.79; N 9.40.

1-(4-Acetylphenyl)-4-(4-chlorophenyl)-1,3-dihydro-2*H*-imidazol-2-one (15)

White solid, yield 3.88 g (62%); m.p. 303–304 °C (1,4-dioxane);

IR (KBr) (ν, cm^{-1}): 1673, 1697 (2 C=O), 3140 (NH);

^{1}H NMR (400 MHz, DMSO-d_6) δ (ppm): 2.59 (s, 3 H, CH_3), 7.49 (d, 2 H, J=8.1 Hz, H_{Ar}), 7.69 (d, 2 H, J=8.1 Hz, H_{Ar}), 7.86 (s, 1H, CH), 8.04 (q, 2 H, J=8.6 Hz, H_{Ar}), 11.27 (s, 1H, NH);

^{13}C NMR (101 MHz, DMSO-d_6) δ (ppm): 26.64 (CH_3), 106.82, 119.26, 122.12, 125.16, 127.73, 128.86, 129.48, 131.64, 133.03, 140.97 (C_{Ar}), 152.31 (NC=O), 196.76 (CH_3C=*O*);

HRMS (ESI): *m/z* calcd. for $C_{17}H_{14}ClN_2O_2$ 313.0744; found: 313.0730 $[M+H]^+$.

1-(4-Acetylphenyl)-4-(4-hydroxyphenyl)-1,3-dihydro-2*H*-imidazol-2-one (16)

Light green solid, yield 5.53 g (94%); m.p. 312–313 °C (DMF);

IR (KBr) (ν, cm^{-1}):1599, 1676 (C=O), 3143 (OH), 3377 (NH);

^{1}H NMR (400 MHz, DMSO-d_6) δ (ppm): 2.58 (s, 3 H, CH_3), 6.80 (d, 2 H, J=8.0 Hz, H_{Ar}), 7.48 (d, 2 H, J=8.0 Hz, H_{Ar}), 7.54 (s, 1H, CH), 8.03 (s, 4 H, H_{Ar}), 9.75 (br. s, 1H, OH), 11.05 (s, 1H, NH);

^{13}C NMR (101 MHz, DMSO-d_6) δ (ppm): 26.60 (CH_3), 103.51, 115.59, 118.91, 119.73, 123.68, 125.16, 129.47, 132.63, 141.29, 152.37, 157.07 (NC=O, C_{Ar}), 196.71 (CH_3C=*O*);

Calcd. for C17H15N2O3, %: C 69.14; H 5.12; N 9.49. Found, %: C 69.04; H 5.11; N 9.51.

1-(4-Acetylphenyl)-4-(4-nitrophenyl)-1,3-dihydro-2*H*-imidazol-2-one (17)

Orange solid, yield 5.56 g (86%); m.p. 292–293 °C (methanol);

IR (KBr) (ν, cm^{-1}): 1711, 1678 (2 C=O), 3134 (NH);

^{1}H NMR (400 MHz, DMSO-d_6) δ (ppm): 2.59 (s, 3 H, CH_3), 7.89 (d, 2 H, J=8.7 Hz, H_{Ar}), 8.01 (d, 2 H, J=8.7 Hz, H_{Ar}), 8.06 (d, 2 H, J=8.7 Hz, H_{Ar}), 8.15 (s, 1H, CH), 8.26 (d, 3 H, J=8.7 Hz, H_{Ar}), 11.48 (s, 1H, NH);

^{13}C NMR (101 MHz, DMSO-d_6) δ (ppm): 26.66 (CH_3), 110.52, 119.65, 121.40, 123.91, 124.32, 129.47, 133.42, 135.25, 140.62, 145.62 (C_{Ar}), 152.29 (NC=O), 196.79 (CH_3C=*O*);

Calcd. for $C_{17}H_{14}N_3O_4$, %: C 62.96; H 4.35; N 12.96. Found, %: C 63.10; H 4.37; N 12.92.

1-(4-(1-(Hydroxyimino)ethyl)phenyl)-4-phenyl-1,3-dihydro-2*H*-imidazole-2-thione **(18)** was prepared from compound **8** according to the procedure of the synthesis of oxime **7**.

White solid, yield 0.59 g (95%); m.p. 310–311 °C (1,4-dioxane);

IR (KBr) (ν, cm^{-1}): 1288 (C=S), 3044 (NH), 3145 (OH);

^{1}H NMR (400 MHz, DMSO-d_6) δ (ppm): 2.21 (s, 3 H, CH_3), 7.32 (t, 1H, J=7.3 Hz, H_{Ar}), 7.43 (d, 2 H, J=7.6 Hz, H_{Ar}), 7.65–7.87 (m, 6 H, H_{Ar}), 7.89 (s, 1H, CH), 11.36 (s, 1H, OH), 13.00 (s, 1H, NH);

^{13}C NMR (101 MHz, DMSO-d_6) δ (ppm): 11.58 (CH_3), 115.63, 124.25, 125.63, 125.89, 128.46, 128.93, 136.30, 127.82, (C_{Ar}), 152.35 (C=NOH), 162.61 (C=S);

HRMS (ESI): *m/z* calcd. for $C_{17}H_{16}N_3OS$ 310.1014; found: 310.1007 $[M+H]^+$.

General procedure for the synthesis of 19–23.

To a solution of the corresponding 2-thioimidazole **8–12** (1.7 mmol) in DMF (3 mL) triethylamine (0.61 g, 6 mmol) and ethyl iodide (1.33 g, 8.5 mmol) were added dropwise, and the reaction mixture was stirred at room temperature for 1 h. Then volatile fractions were separated under reduced pressure and obtained residue was diluted with water (5 mL). The formed precipitate was filtered off, washed with propan-2-ol, dried and recrystallized from propan-2-ol to afford compounds **19–23**.

1-(4-(2-(Ethylthio)-4-phenyl-1*H*-imidazol-1-yl)phenyl)ethan-1-one (19)

White solid, yield 0.53 g (97%); m.p. 88–89 °C;

IR (KBr) (ν, cm^{-1}): 1682 (C=O);

^{1}H NMR (400 MHz, DMSO-d_6) δ (ppm): 1.28 (t, 3 H, J = 7.1 Hz, CH_2CH_3), 2.64 (s, 3 H, CH_3), 3.10 (q, 2 H, J = 7.0 Hz, CH_2CH_3), 7.24 (t, 1H, J = 7.2 Hz, H_{Ar}), 7.39 (t, 2 H, J = 7.3 Hz, H_{Ar}), 7.67 (d, 2 H, J = 7.5 Hz, H_{Ar}), 7.84 (d, 2 H, J = 7.6 Hz, H_{Ar}), 8.09 (s, 1H, CH), 8.12 (d, 2 H, J = 7.5 Hz, H_{Ar});

^{13}C NMR (101 MHz, DMSO-d_6) δ (ppm): 14.79 (CH_2CH_3), 26.87, 27.56 (CH_2CH_3, CH_3), 118.63, 124.38, 125.09, 126.85, 128.57, 129.51, 133.43, 136.09, 140.35, 141.45, 141.67 (C_{Ar}), 197.03 (C = O);

HRMS (ESI): m/z calcd. for $C_{19}H_{19}N_2OS$ 323.1218; Found: 323.1209 $[M+H]^+$.

1-(4-(2-(Ethylthio)-4-(4-fluorophenyl)-1*H*-imidazol-1-yl)phenyl)ethan-1-one (20)

White solid, yield 0.56 g (96%); m.p. 138−139 °C;

IR (KBr) (ν, cm^{-1}): 1676 (C = O);

^{1}H NMR (400 MHz, DMSO-d_6) δ (ppm): 1.29 (t, 3 H, J = 7.3 Hz, CH_2CH_3), 2.64 (s, 3 H, CH_3), 3.14 (q, 2 H, J = 7.3 Hz, CH_2CH_3), 7.23 (t, 2 H, J = 8.8 Hz, H_{Ar}), 7.67 (d, 2 H, J = 8.3 Hz, H_{Ar}), 7.87 (dd, 2 H, J = 8.1, 5.8 Hz, H_{Ar}), 8.08 (s, 1H, CH), 8.13 (d, 2 H, J = 8.3 Hz, H_{Ar});

^{13}C NMR (101 MHz, DMSO-d_6) δ (ppm): 14.79 (CH_2CH_3), 26.88, 27.54 (CH_2CH_3, CH_3), 115.45 (d, J = 21.5 Hz), 118.49, 125.09, 126.26 (d, J = 8.0 Hz), 129.54, 130.03 (d, J = 2.9 Hz), 136.14, 140.32, 140.58, 141.78, 161.26 (d, J = 243.3 Hz) (C_{Ar}), 197.06 (C = O);

HRMS (ESI): m/z calcd. for $C_{19}H_{18}FN_2OS$ 341.1124; found: 341.1116 $[M+H]^+$.

1-(4-(4-(4-Chlorophenyl)-2-(ethylthio)-1*H*-imidazol-1-yl)phenyl)ethan-1-one (21)

White solid, yield 0.58 g (97%); m.p. 125−126 °C;

IR (KBr) (ν, cm^{-1}): 1674 (C = O); ^{1}H NMR (400 MHz, DMSO-d_6) δ (ppm): 1.29 (t, 3 H, J = 7.3 Hz, CH_2CH_3), 2.64 (s, 3 H, CH_3), 3.15 (q, 2 H, J = 7.3 Hz, CH_2CH_3), 7.46 (d, 2 H, J = 8.2 Hz, H_{Ar}), 7.67 (d, 2 H, J = 8.2 Hz, H_{Ar}), 7.85 (d, 2 H, J = 8.2 Hz, H_{Ar}), 8.13 (d, 2 H, J = 8.2 Hz, H_{Ar}), 8.15 (s, 1H, CH);

^{13}C NMR (101 MHz, DMSO-d_6) δ (ppm): 14.78 (CH_2CH_3), 26.89, 27.50 (CH_2CH_3, CH_3), 119.17, 125.13, 126.02, 128.63, 129.54, 131.13, 132.38, 136.20, 140.25, 140.29, 142.07 (C_{Ar}), 197.06 (C = O);

HRMS (ESI): m/z calcd. for $C_{19}H_{18}ClN_2OS$ 357.0828; found: 357.0823 $[M+H]^+$.

1-(4-(2-(Ethylthio)-4-(4-hydroxyphenyl)-1*H*-imidazol-1-yl)phenyl)ethan-1-one (22)

Light pink solid, yield 0.55 g (95%); m.p. 219−220 °C;

IR (KBr) (ν, cm^{-1}): 1683 (C = O), 2924 (OH);

^{1}H NMR (400 MHz, DMSO-d_6) δ (ppm): 1.27 (t, 3 H, J = 7.3 Hz, CH_2CH_3), 2.64 (s, 3 H, CH_3), 3.11 (q, 2 H, J = 7.3 Hz, CH_2CH_3), 6.78 (d, 2 H, J = 8.5 Hz, H_{Ar}), 7.65 (dd, 4 H, J = 8.2, 6.9 Hz, H_{Ar}), 7.88 (s, 1H, CH), 8.12 (d, 2 H, J = 8.5 Hz, H_{Ar}), 9.42 (s, 1H, OH);

^{13}C NMR (101 MHz, DMSO-d_6) δ (ppm): 14.82 (CH_2CH_3), 26.88, 27.61 (CH_2CH_3, CH_3), 115.34, 116.84, 124.60, 125.10, 125.80, 129.51, 135.94, 140.53, 140.96, 141.91, 151.33, 156.56 (C_{Ar}), 197.07 (C = O);

HRMS (ESI): m/z calcd. for $C_{19}H_{19}N_2O_2S$ 339.1167; found: 339.1161 $[M+H]^+$.

1-(4-(2-(Ethylthio)-4-(4-nitrophenyl)-1*H*-imidazol-1-yl)phenyl)ethan-1-one (23)

Orange solid, yield 0.61 g (98%); m.p. 146−147 °C;

IR (KBr) (ν, cm^{-1}): 1680 (C = O);

^{1}H NMR (400 MHz, DMSO-d_6) δ (ppm): 1.31 (t, 3 H, J = 7.3 Hz, CH_2CH_3), 2.65 (s, 3 H, CH_3), 3.18 (q, 2 H, J = 7.3 Hz, CH_2CH_3), 7.70 (d, 2 H, J = 8.4 Hz, H_{Ar}), 8.07 (d, 2 H, J = 8.7 Hz, H_{Ar}), 8.14 (d, 2 H, J = 8.4 Hz, H_{Ar}), 8.27 (d, 2 H, J = 8.7 Hz, H_{Ar}), 8.41 (s, 1H, CH);

^{13}C NMR (101 MHz, DMSO-d_6) δ (ppm): 14.74 (CH_2CH_3), 26.91, 27.42 (CH_2CH_3, CH_3), 121.90, 124.25, 124.87, 125.23, 129.60, 136.45, 139. 38, 140.02, 143.39, 145.73, 159.11 (C_{Ar}), 197.08 (C = O);

HRMS (ESI): m/z calcd. for $C_{19}H_{18}N_3O_3S$: Calcd.: 368.1069; found: 368.1060 $[M+H]^+$.

General procedure for the synthesis of 24–26.

To a solution of the corresponding imidazole **13**, **15 11** and (1.5 g, 5.4 mmol) in DMF (3 mL) grounded KOH (0.6 g, 10.8 mmol) and K_2CO_3 (1.49 g, 10.8 mmol) were added to the solution and the mixture was stirred at room temperature for 10 min. Then ethyl iodide (3.37 g, 21.6 mmol) was added dropwise and the reaction mixture was stirred at room temperature for 1 h. After completion of the reaction, volatile fractions were separated under reduced pressure and obtained residue was diluted with water. The formed precipitate was filtered off, washed with water, propan-2-ol, dried, and recrystallized from 2-propanol to afford compounds **24–26**.

1-(4-Acetylphenyl)-3-ethyl-4-phenyl-1,3-dihydro-2*H*-imidazol-2-one (24)

White solid, yield 1.14 g (69%); m.p. 110–111 °C);

IR (KBr) (ν, cm^{-1}): 1667, 1689, (2 C = O);

^{1}H NMR (400 MHz, DMSO-d_6) δ (ppm): 1.09 (t, 3 H, J = 7.1 Hz, CH_2CH_3), 2.59 (s, 3 H, CH_3), 3.77 (q, 2 H, J = 7.0 Hz, CH_2CH_3), 7.41 (s, 1H, H_{Ar}), 7.47–7.42 (m, 1H, H_{Ar}), 7.50 (d, 2 H, J = 7.6 Hz, H_{Ar}), 7.53–7.54 (m, 1H, H_{Ar}), 7.56 (s, 1H, CH), 8.09–7.99 (m, 4 H, H_{Ar});

^{13}C NMR (101 MHz, DMSO-d_6) δ (ppm): 14.74 (CH_2CH_3), 27.11 (CH_3), 36.88 (CH_2CH_3), 107.13 (CH), 119.83 (CN), 126.01, 128.26, 128.99, 129.45, 129.97, 133.59, 141.40 (C_{Ar}), 151.86 (C = O), 197.23 ($CH_3C=O$);

HRMS (ESI) $C_{19}H_{19}N_2O_2$: Calcd.: 307.1446; Found: 307.1438 $[M+H]^+$.

1-(4-Acetylphenyl)-4-(4-chlorophenyl)-3-ethyl-1,3-dihydro-2*H*-imidazol-2-one (25)

Yellowish solid, yield 1.80 g (98%); m.p. 185–186 °C;

IR (KBr) (ν, cm^{-1}): 1706, 1664 (2 C = O);

^{1}H NMR (400 MHz, DMSO-d_6) δ (ppm): 1.08 (t, 3 H, J = 7.1 Hz, CH_2CH_3), 2.59 (s, 3 H, CH_3), 3.76 (q, 2 H, J = 7.0 Hz, CH_2CH_3), 7.47 (s, 1H, H_{Ar}), 7.58 (s, 4 H, H_{Ar}, CH), 8.03 (q, 4 H, J = 8.8 Hz, H_{Ar});

^{13}C NMR (101 MHz, DMSO-d_6) δ (ppm): 14.74 (CH_2CH_3), 27.11 (CH_3), 36.91 (CH_2CH_3), 107.74 (CH), 119.91 (CN), 124.80, 128.30, 129.51, 129.91, 129.97, 133.60, 133.69, 141.28 (C_{Ar}), 151.74 (C = O), 197.24 ($CH_3C=O$);

HRMS (ESI) $C_{19}H_{18}ClN_2O_2$: Calcd.: 341.1047; Found: 341.1046 $[M+H]^+$.

1-(4-(4-(4-Ethoxyphenyl)-2-(ethylthio)-1*H*-imidazol-1-yl)phenyl)ethan-1-one (26)

White solid, yield 1.72 g (87%); m.p. 92−91 °C;

IR (KBr) (ν, cm^{-1}): 1677 (C = O);

^{1}H NMR (400 MHz, DMSO-d_6) δ (ppm): 1.28 (t, 3 H, J = 7.3, CH_2CH_3), 1.34 (t, 3 H, J = 6.9, CH_2CH_3), 2.64 (s, 3 H, CH_3), 3.12 (q, 2 H, J = 7.3 Hz, CH_2CH_3), 4.04 (q, 2 H, J = 6.9 Hz, CH_2CH_3) 6.95 (d, 2 H, J = 8.6 Hz, H_{Ar}), 7.66 (d, 2 H, J = 8.4 Hz, H_{Ar}), 7.74 (d, 2 H, J = 8.6 Hz, H_{Ar}) 7.96 (s, 1H, CH), 8.12 (d, 2 H, J = 8.4 Hz, H_{Ar});

^{13}C NMR (101 MHz, DMSO-d_6) δ (ppm): 14.69, 14.80 ($2CH_2CH_3$), 26.87, 27.59 (CH_2CH_3, CH_3), 62.98 (OCH_2CH_3), 114.45, 117.34, 125.02, 125.71, 126.03, 129.51, 135.98, 140.47, 141.22, 141.50, 157.65 (C_{Ar}), 197.05 (C = O);

HRMS (ESI): *m/z* calcd. for $C_{21}H_{23}N_2O_2S$ 367.1480; found: 367.1477 $[M+H]^+$.

Cell culturing

The human triple-negative breast cancer MDA-MB-231 and human glioblastoma U-87 cell lines were obtained from the American Type Culture Collection (ATCC, Manassas, VA, USA). Human foreskin fibroblasts (HF) CRL-4001 were originally obtained from ATCC and kindly provided by Prof. Helder Santos (University of Helsinki, Finland). Primary prostate carcinoma PPC-1 cell line was kindly provided by Prof. Tambet Teesalu (University of Tartu, Estonia). MDA-MB-231, PPC-1, U-87 and HF were cultured in Dulbecco's Modified Eagle's GlutaMAX medium (Gibco (Carlsbad, CA, USA)), which was supplemented with 10,000 U/mL penicillin, 10 mg/mL streptomycin (Gibco), and 10% fetal bovine serum (Gibco). This cell growth medium was used for all the biological assays described in this paper. Cell cultures were grown at 37 °C in a humidified atmosphere containing 5% CO_2. They were used until the passage of 20 to avoid the accumulation of genetic and phenotypic changes over time.

Cell viability assay

The compound effect on cell viability was established using 3-(4,5-dimethylthiazol-2-yl)-2,5-diphenyltetrazolium bromide (MTT; Sigma-Aldrich Co., St Louis, MO, USA) assay, as described elsewhere[58]. Briefly, MDA-MB-231, PPC-1, U-87 and HF cells were seeded in 96-well plates (Corning) in triplicates at a volume of 100 µL (MDA-MB-231, PPC1: 4×10^3 cells/well; U-87: 5×10^3 cells/well). After 24 h, the cells were treated with 100 µM of tested compounds. After 72 h, the MTT reagent was added, and cells were incubated for 4 h. Then the medium was aspirated, and 100 µL of DMSO (Sigma-Aldrich Co., St. Louis, MO, USA) was added to each well. The absorbance was measured at 570 and 630 nm using a multi-detection microplate reader. The compound effect on cell viability was calculated using a formula:

$$Relative\ cell\ viability\ (\%) = \frac{A - A_0}{A_{NC} - A_0}$$

Where:

A – mean of absorbance of tested compound,

A_0 – mean of absorbance of blank (no cells, positive control),

A_{NC} – mean of absorbance of negative control (only cells, no treatment).

The EC_{50} values of the most active imidazole derivatives 3, 8, 13, and 21 was established by the same MTT procedure. The compound serial dilutions from 100 µM to 1.56 µM have been made in a medium and added to the cells in triplicates. EC_{50} value that represents the concentration of a compound causing a 50% reduction of cancer cell metabolic activity has been calculated using the Hill equation.

'Wound healing' assay

The compound effect on PPC-1 and U-87 cell migration was tested by a 'wound healing' assay, as described elsewhere[59]. Briefly, human prostate carcinoma PPC-1 and glioblastoma U-87 cells were seeded in 24-well plates at a density of 6×10^4 cells/well and incubated for 48–72 h in cell culture medium at 37 °C in a humidified atmosphere containing 5% CO_2, until cell monolayer was formed. Then, in the center of each well, the scratch was made using a 100 µl pipette tip. The cells were washed gently with PBS, and the fresh medium containing compound concentration corresponding to 50% of their established EC_{50} values was added. Medium containing 0.2% DMSO was used as a negative control. The cells were incubated at 37 °C in a humidified atmosphere containing 5% CO_2. 'Wounds' were captured at intervals of 0 h, 24 h, 48 h, 72 h (for PPC-1 cell line), and 0 h, 12 h, 24 h (for U-87 cell line) under phase contrast microscopy at a 4× magnification. The 'wound' area was analysed using the ImageJ program (National Institutes of Health).

Compound activity in cell 3D cultures (spheroids)

Cancer cell spheroids were formed by using the magnetic 3D Bioprinting method, as described elsewhere[51]. Briefly, triple-negative breast cancer MDA-MB-231 cells, prostate carcinoma PPC-1, glioblastoma U-87 and human fibroblasts at 70% confluency in a 6-well plate were incubated with Nanoshuttle (n3D Biosciences, Inc.) for 8 h. Then, cells were trypsinized, centrifuged and seeded into an ultra-low attachment 96-well plate in a volume

of 100 µL (1.5×10^3 cancer cells and 1.5×10^3 human fibroblasts/well). The plate was placed on a magnetic drive and incubated for 2 days at 37 °C in the incubator. Then, the fresh medium containing 10 µM of compounds **4**, **9**, **14** and **22** was added to the wells. The spheroids were captured every two days using the Olympus IX73 inverted microscope (Olympus Corporation). The quantitative analysis of compound anticancer activity in spheroids was performed using ImageJ (National Institute of Health and Microsoft Office Excel software).

After 8 days of incubation, 20 µl of MTT reagent was added to each well. After 12 h of incubation, the medium was aspirated. 100 µl of DMSO was added to each well and incubated overnight in the fridge, protected from light. Then, the absorbance was measured at 570 and 630 nm using a multi-detection microplate reader. Spheroid cell viability was calculated using a formula provided in Sect. 4.4.

Statistical analysis

All biological experiments were repeated at three times, calculating the mean and standard deviation. The data was processed using Microsoft Office Excel 2016 software (Microsoft Corporation, Redmond, WA, USA). Statistical analysis was performed by using Student's t-test. The level of significance was set as $p < 0.05$.

Data availability

All data generated during this study are included in this article and its supplementary information file.

Received: 29 July 2024; Accepted: 15 October 2024
Published online: 14 November 2024

References

1. Cancer cases and deaths on the rise in the EU - European Commission [Internet]. [cited 2024 Jun 11]. (2024). https://joint-research-centre.ec.europa.eu/jrc-news-and-updates/cancer-cases-and-deaths-rise-eu-2023-10-02_en
2. Pérez-Herrero, E. & Fernández-Medarde, A. Advanced targeted therapies in cancer: drug nanocarriers, the future of chemotherapy. *Eur. J. Pharm. Biopharm.* **93**, 52–79 (2015).
3. Tolomeu, H. V., Fraga, C. A. M. & Imidazole Synthesis, functionalization and Physicochemical Properties of a Privileged structure in Medicinal Chemistry. *Molecules.* **28** (2), 838 (2023).
4. Hill, R. A. 5 Marine natural products. *Annu. Rep. Prog Chem. Sect. B.* **99**, 183 (2003).
5. Forte, B. et al. A submarine journey: the pyrrole-imidazole alkaloids. *Mar. Drugs.* **7** (4), 705–753 (2009).
6. Jin, Z. Muscarine, imidazole, oxazole, and thiazole alkaloids. *Nat. Prod. Rep.* **28** (6), 1143 (2011).
7. Gao, G. et al. Efficient imidazolium catalysts for the Benzoin Condensation. *J. Chem. Res.* **2002** (6), 262–263 (2002).
8. Nasrollahzadeh, M. S. et al. Design, synthesis and biological evaluation of novel imidazole-based benzamide and hydroxamic acid derivatives as potent histone deacetylase inhibitors and anticancer agents. *J. Mol. Struct.* **1297**, 136951 (2024).
9. Dacarbazine Monograph for Professionals [Internet]. Drugs.com. [cited 2024 Jun 11]. https://www.drugs.com/monograph/dacarbazine.html
10. Alghamdi, S. S., Suliman, R. S., Almutairi, K., Kahtani, K. & Aljatli, D. Imidazole as a Promising Medicinal Scaffold: current status and future direction. *DDDT.* **15**, 3289–3312 (2021).
11. Aruchamy, B. et al. Imidazole-pyridine hybrids as potent anti-cancer agents. *Eur. J. Pharm. Sci.* **180**, 106323 (2023).
12. Ali, I., Lone, M. N. & Aboul-Enein, H. Y. Imidazoles as potential anticancer agents. *Med. Chem. Commun.* **8** (9), 1742–1773 (2017).
13. Gudipudi, G., Sagurthi, S. R., Perugu, S., Achaiah, G. & David Krupadanam, G. L. Rational design and synthesis of novel 2-(substituted-2H-chromen-3-yl)-5-aryl-1H-imidazole derivatives as an anti-angiogenesis and anti-cancer agent. *RSC Adv.* **4** (99), 56489–56501 (2014).
14. Dao, P. et al. Design, synthesis, and evaluation of Novel Imidazo[1,2- *a*][1,3,5]triazines and their derivatives as focal adhesion kinase inhibitors with Antitumor Activity. *J. Med. Chem.* **58** (1), 237–251 (2015).
15. Baviskar, A. T. et al. N-Fused Imidazoles as Novel Anticancer agents that Inhibit Catalytic Activity of Topoisomerase IIα and induce apoptosis in G1/S phase. *J. Med. Chem.* **54** (14), 5013–5030 (2011).
16. Torres, F. et al. Imidazoles and Benzimidazoles as Tubulin-modulators for Anti-cancer Therapy. *CMC.* **22** (11), 1312–1323 (2015).
17. Frühauf, A., Behringer, M. & Meyer-Almes, F. J. Significance of five-Membered heterocycles in human histone deacetylase inhibitors. *Molecules.* **28** (15), 5686 (2023).
18. Sharma, P., LaRosa, C., Antwi, J., Govindarajan, R. & Werbovetz, K. A. Imidazoles as potential Anticancer agents: an update on recent studies. *Molecules.* **26** (14), 4213 (2021).
19. Afifi, N. & Barrero, C. A. Understanding breast Cancer aggressiveness and its implications in diagnosis and treatment. *JCM.* **12** (4), 1375 (2023).
20. Obidiro, O., Battogtokh, G. & Akala, E. O. Triple negative breast Cancer Treatment options and limitations: Future Outlook. *Pharmaceutics.* **15** (7), 1796 (2023).
21. Stupp, R. et al. Radiotherapy plus Concomitant and Adjuvant Temozolomide for Glioblastoma. *N Engl. J. Med.* **352** (10), 987–996 (2005).
22. Roda, D., Veiga, P., Melo, J. B., Carreira, I. M. & Ribeiro, I. P. Principles in the management of Glioblastoma. *Genes.* **15** (4), 501 (2024).
23. Bray, F. et al. Global cancer statistics 2018: GLOBOCAN estimates of incidence and mortality worldwide for 36 cancers in 185 countries. *CA Cancer J. Clin.* **68** (6), 394–424 (2018).
24. Posdzich, P. et al. Metastatic prostate Cancer—A Review of Current Treatment options and Promising New approaches. *Cancers.* **15** (2), 461 (2023).
25. Vessally, E., Saeidian, H., Hosseinian, A., Edjlali, L. & Bekhradnia, A. A review on synthetic applications of Oxime Esters. *COC.* **21** (3), 249–271 (2016).
26. Yu, F. et al. Pharmacological characterization of oxime agonists of the histamine H4 receptor. *JRLCR.* 2010:**3**, 37–49 (2009).
27. Kassa, J., Kuca, K., Karasova, J. & Musilek, K. The development of New Oximes and the evaluation of their reactivating, therapeutic and neuroprotective efficacy against Tabun. *MRMC.* **8** (11), 1134–1143 (2008).
28. Mohamed, A. H. et al. New imidazole-2-thiones linked to acenaphythylenone as dual DNA intercalators and topoisomerase II inhibitors: structural optimization, docking, and apoptosis studies. *J. Enzyme Inhib. Med. Chem.* **39** (1), 2311818 (2024).
29. Ibrahim, S. A., Al-Mhyawi, S. R. & Atlam, F. M. New imidazole-2-ones and their 2-thione analogues as anticancer agents and CAIX inhibitors: synthesis, in silico ADME and molecular modeling studies. *Bioorg. Chem.* **141**, 106872 (2023).
30. Xue, N. et al. Synthesis and biological evaluation of imidazol-2-one derivatives as potential antitumor agents. *Bioorg. Med. Chem.* **16** (5), 2550–2557 (2008).
31. Li, N. et al. Discovery of Novel Celastrol–Imidazole derivatives with Anticancer Activity *in Vitro* and *in vivo*. *J. Med. Chem.* **65** (6), 4578–4589 (2022).

32. Yadav, S. et al. Synthesis and evaluation of antimicrobial, antitubercular and anticancer activities of 2-(1-benzoyl-1H-benzo[d] imidazol-2-ylthio)-N-substituted acetamides. *Chem. Cent. J.* **12** (1), 66 (2018).
33. Özkay, Y., Işıkdağ, İ., İncesu, Z. & Akalın, G. Synthesis of 2-substituted-N-[4-(1-methyl-4,5-diphenyl-1H-imidazole-2-yl)phenyl] acetamide derivatives and evaluation of their anticancer activity. *Eur. J. Med. Chem.* **45** (8), 3320–3328 (2010).
34. Balandis, B., Mickevičius, V. & Petrikaitė, V. Exploration of Benzenesulfonamide-Bearing imidazole derivatives activity in Triple-negative breast Cancer and melanoma 2D and 3D cell cultures. *Pharmaceuticals*. **14** (11), 1158 (2021).
35. Han, S. J., Kwon, S. & Kim, K. S. Challenges of applying multicellular tumor spheroids in preclinical phase. *Cancer Cell. Int.* **21** (1), 152 (2021).
36. Kim, B., Ram, S., Hyeon, G., Kim, J. J. & Yoon, Y. J. A development of Rapid, practical and selective process for Preparation of Z-Oximes. *J. Korean Chem. Soc.* **57** (2), 295–299 (2013).
37. Esteban, J., Costa, A. M., Urpí, F. & Vilarrasa, J. From (E)- and (Z)-ketoximes to N -sulfenylimines, ketimines or ketones at will. Application to erythromycin derivatives. *Tetrahedron Lett.* **45** (29), 5563–5567 (2004).
38. Šermukšnytė, A., Kantminienė, K., Jonuškienė, I., Tumosienė, I. & Petrikaitė, V. The Effect of 1,2,4-Triazole-3-thiol derivatives bearing Hydrazone Moiety on Cancer Cell Migration and Growth of Melanoma, breast, and pancreatic Cancer spheroids. *Pharmaceuticals*. **15** (8), 1026 (2022).
39. Zubrickė, I., Jonuškienė, I., Kantminienė, K., Tumosienė, I. & Petrikaitė, V. Synthesis and in Vitro evaluation as potential anticancer and antioxidant agents of diphenylamine-pyrrolidin-2-one-hydrazone derivatives. *IJMS*. **24** (23), 16804 (2023).
40. Cailleau, R., Young, R., Olivé, M. & Reeves, W. J. Breast Tumor Cell Lines from Pleural Effusions2. JNCI. *J. Natl Cancer Inst.* **53** (3), 661–674 (1974).
41. Shaheen, S., Fawaz, F., Shah, S. & Büsselberg, D. Differential expression and pathway analysis in drug-resistant triple-negative breast Cancer cell lines using RNASeq analysis. *IJMS*. **19** (6), 1810 (2018).
42. Chavez, K. J., Garimella, S. V. & Lipkowitz, S. Triple negative breast cancer cell lines: One tool in the search for better treatment of triple negative breast cancer. Eng-Wong J, Zujewski JA, editors. BD. ;32(1–2):35–48. (2011).
43. Elkaeed, E. B., Salam, H. A. A. E., Sabt, A., Al-Ansary, G. H. & Eldehna, W. M. Recent advancements in the development of Anti-breast Cancer Synthetic Small molecules. *Molecules*. **26** (24), 7611 (2021).
44. Junaid, A., Lim, F. P. L., Chuah, L. H. & Dolzhenko, A. V. 6, N^2 -Diaryl-1,3,5-triazine-2,4-diamines: synthesis, antiproliferative activity and 3D-QSAR modeling. RSC Adv. ;10(21):12135–44. (2020).
45. Yu, S. et al. fang, hong, hong,. Isolation and characterization of cancer stem cells from a human glioblastoma cell line U87. Cancer Letters. ;265(1):124–34. (2008).
46. Poon, M. T. C., Bruce, M., Simpson, J. E., Hannan, C. J. & Brennan, P. M. Temozolomide sensitivity of malignant glioma cell lines – a systematic review assessing consistencies between in vitro studies. *BMC Cancer*. **21** (1), 1240 (2021).
47. Brothman, A. R., Wilkins, P. C., Sales, E. W. & Somers, K. D. Metastatic properties of the human Prostatic Cell line, PPC-1, in athymic nude mice. *J. Urol.* **145** (5), 1088–1091 (1991).
48. Jeong, S. Y., Lee, J. H., Shin, Y., Chung, S. & Kuh, H. J. Co-Culture of Tumor Spheroids and Fibroblasts in a Collagen Matrix-Incorporated Microfluidic Chip Mimics Reciprocal Activation in Solid Tumor Microenvironment. Lee JW, editor. PLoS ONE. ;11(7):e0159013. (2016).
49. Petrikaite, V., D'Avanzo, N., Celia, C. & Fresta, M. Nanocarriers overcoming biological barriers induced by multidrug resistance of chemotherapeutics in 2D and 3D cancer models. *Drug Resist. Updates*. **68**, 100956 (2023).
50. Daunys, S., Janonienė, A., Januškevičienė, I., Paškevičiūtė, M. & Petrikaitė, V. 3D Tumor Spheroid models for in Vitro Therapeutic Screening of nanoparticles. *Adv. Exp. Med. Biol.* **1295**, 243–270 (2021).
51. Bytautaite, M. & Petrikaite, V. Comparative study of lipophilic statin activity in 2D and 3D in vitro models of human breast Cancer cell lines MDA-MB-231 and MCF-7. *Onco Targets Ther.* **13**, 13201–13209 (2020).
52. Zanoni, M. et al. 3D tumor spheroid models for in vitro therapeutic screening: a systematic approach to enhance the biological relevance of data obtained. *Sci. Rep.* **6** (1), 19103 (2016).
53. Dzobo, K. & Dandara, C. The Extracellular Matrix: its composition, function, remodeling, and role in Tumorigenesis. *Biomimetics*. **8** (2), 146 (2023).
54. Habanjar, O., Diab-Assaf, M., Caldefie-Chezet, F. & Delort, L. 3D cell Culture systems: Tumor Application, advantages, and disadvantages. *IJMS*. **22** (22), 12200 (2021).
55. Satpathy, A. et al. Developments with 3D bioprinting for novel drug discovery. *Expert Opin. Drug Discov.* **13** (12), 1115–1129 (2018).
56. Zaraei, S. O. et al. Discovery of first-in-class imidazothiazole-based potent and selective ErbB4 (HER4) kinase inhibitors. *Eur. J. Med. Chem.* **224**, 113674 (2021).
57. Ali, E. M. H. et al. Design, synthesis, and biological evaluation of novel imidazole derivatives possessing terminal sulphonamides as potential BRAFV600Einhibitors. *Bioorg. Chem.* **106**, 104508 (2021).
58. Čeponytė, U., Paškevičiūtė, M. & Petrikaitė, V. Comparison of NSAIDs activity in COX-2 expressing and non-expressing 2D and 3D pancreatic cancer cell cultures. *Cancer Manag Res.* **10**, 1543–1551 (2018).
59. Skaraitė, I., Maccioni, E. & Petrikaitė, V. Anticancer activity of Sunitinib analogues in Human pancreatic Cancer cell cultures under Normoxia and Hypoxia. *IJMS*. **24** (6), 5422 (2023).

Author contributions

Conceptualization, V.M. and V.P.; methodology, V.M. and V.P.; formal analysis, B.G., U.E., and V.P.; investigation, B.G., R.V., U.E., and V.P.; resources, V.M. and V.P.; writing—original draft preparation, B.G., V.M. and V.P.; writing—review and editing, V.M. and V.P.; visualization, B.G., U.E. and V.P.; supervision, V.M. and V.P.; funding acquisition, V.M. and V.P. All authors have read and agreed to the submitted version of the manuscript.

Declarations

Competing interests

The authors declare no competing interests.

Informed consent

Not applicable.

Additional information

Supplementary Information The online version contains supplementary material available at https://doi.org/10.1038/s41598-024-76533-4.

Correspondence and requests for materials should be addressed to V.M. or V.P.